Atomic-Oxygen-Flow Generation by Laser-Driven Plasma Wind Tunnel as Low-Earth-Orbit-Environment Simulator

Atomic-Oxygen-Flow Generation by Laser-Driven Plasma Wind Tunnel as Low-Earth-Orbit Environment Simulator

Makoto Matsui[1]
Shizuoka University, Hamamatsu, Shizuoka 432-8561, Japan

Shingo Yoneda[2]
University of Tokyo, Bunkyo, Tokyo 113-8656, Japan

Kimiya Komurasaki[3]
University of Tokyo, Kashiwa, Chiba 277-8561, Japan

Yoshiki Yamagiwa[4]
Shizuoka University, Hamamatsu, Shizuoka 432-8561, Japan

and
Yoshihiro Arakawa[5]
University of Tokyo, Bunkyo, Tokyo 113-8656, Japan

Nomenclature

C_p = specific heat at constant pressure

c = velocity of light

h_{chem} = chemical potential

h_0 = total specific enthalpy

I = probe laser intensity

K = integrated absorption coefficient

k = absorption coefficient

k_B = Boltzmann constant

M_{av} = average molecular weight

m = molecular weight

R = gas constant

r = radial position

T = translational temperature

T^* = throat temperature

[1] Assistant Professor, Department of Mechanical Engineering, 3-5-1 Johoku, Senior Member.
[2] Graduate Student, Department of Aeronautics and Astronautics, 7-3-1 Hongo.
[3] Professor, Department of Advanced Energy, 3-5-1 Kashiwa, Senior Member.
[4] Professor, Department of Mechanical Engineering, 3-5-1 Johoku, Senior Member.
[5] Professor, Department of Aeronautics and Astronautics, 7-3-1 Hongo, Senior Member.

T_{ref} = reference temperature

T_{room} = room temperature

T_0 = total temperature

u = flow velocity

x = position in the laser path

y = distance between the flow axis and the laser path

γ = specific heat ratio

$\Delta\nu_D$ = Doppler width

θ = incident-laser-beam angle to the axis

ν = probe laser frequency

ν_0 = center absorption frequency

ν_c = constant for Gaussian fit

ν_{shift} = Doppler shift

I. Introduction

The main atmospheric component in the low earth orbit (LEO) is atomic oxygen produced in dissociation of molecular oxygen by solar UV radiation [1]. Orbiting satellites in the LEO have a velocity of 7.8 km/s; therefore, the atomic oxygen in the LEO collides with the satellites at a corresponding translational energy of 4.5 eV, resulting in severe degradation of their surface materials [2, 3]. Then, a ground test facility where high-speed atomic oxygen flows can be simulated is necessary for investigating this degradation. Atomic oxygen flows are also necessary for the development of super-LEO satellites [4, 5]. However, despite the fact that the super-LEO satellites provide a new frontier of earth observation missions, they experience severe aerodynamic drag, owing to which a huge amount of propellant is required to retain them in orbit. This problem severely limits the mission term. Therefore, recently, air-breathing hall thrusters or ion engines have been proposed to extend the mission term [6–8].

A currently available unique approach for simulating high-speed atomic oxygen environments in the LEO is laser detonation [9, 10]. However, the operation time of this type of simulator is restricted to several hundred microseconds owing to the use of a pulse laser. This is a crucial problem, particularly for the development of air-breathing thrusters. Then, various types of continuous flow generators have been studied. However, an ion-source-type generator combined with a neutralizer is faced with a problem of a broad energy distribution around 4.5 eV,

which is comparable to the plasma potential [11]. Achieving orbit velocity using an aerodynamic-acceleration-type with radio frequency or microwaves is difficult owing to relatively low total temperature and pressure though their electrodeless heating allows operation using pure oxygen [12, 13]. Further, an aerodynamic-type using an arc-heater is faced with the problem of electrode erosion and resulting flow contamination, as well as the necessity for an inert gas to maintain a stable discharge [14, 15].

To overcome the abovementioned problems, we previously developed a laser-driven wind tunnel that would act as a high-density atomic oxygen generator, by producing laser-sustained plasma (LSP) [16, 17]. In LSP, the plasma is sustained by absorbing the power of a focused laser beam through an inverse bremsstrahlung radiation process between electrons and ions. LSP then offers advantages derived from electrodeless heating, such as clean flows and availability of pure oxygen. Additionally, LSP can be operated at levels higher than the atmosphere.

In this study, a laser-driven plasma wind tunnel was developed as a simulator of continuous atomic oxygen flows in the LEO. This was done as follows. A 2-kW continuous-wave CO_2 laser was used to generate atmospheric pure oxygen and oxygen/helium LSP, and LSP was expanded to a vacuum chamber through a convergent-divergent nozzle to produce stationary high-speed atomic oxygen flows. The flows were characterized by laser absorption spectroscopy (LAS).

II. Laser-driven Plasma Wind Tunnel

Figure 1 shows a schematic of the laser-driven plasma wind tunnel. A continuous-wave CO_2 laser (YB-L200B7T4, Matsushita Electric Industrial Co., Ltd.) was used as the beam source, having a wave length of 10.6 μm. The maximum output power was 2 kW, and the transverse electromagnetic wave (TEM) mode of the laser beam was TEM_{10}. The beam divergence was less than 2 mrad at the laser exit. The beam diameter of 20 mm was magnified by factor of 2.2 using a ZnSe beam expander to decrease the F number because the LSP is produced more stably with the decrease in the F number. The expanded beam was then condensed into an LSP generator through a plano convex lens with a focal length of 95 mm and F number of 2.2. This lens can move back to forth in the direction of the laser beam through a traverse stage.

The LSP generator was composed of a laser induction window, plasma-sustaining channel, and convergent-divergent nozzle. The nozzle throat was made of copper and its diameter was varied as described below, whereas the nozzle diameter was fixed to 5 mm. A working gas was blown onto the induction window surface to cool it. An

ignition rod made of stainless steal (SUS304) was used as a source of initial electron emission. After the ignition, the LSP was moved toward the nozzle throat by changing the position of the focal lens.

The generator was connected to a water-cooled vacuum chamber having two quartz windows for access to an expanded plume by optical diagnostics. With parallel operation of two mechanical booster pumps (MBP; ULVAC, Inc., PRC012A; 1000 m3/h) and two rotary pumps (RP; ULVAC, Inc., VS1501, 150 m3/h), the ambient pressure and mass flow rate of oxygen could be maintained less than 50 Pa and less than 5 slm, respectively.

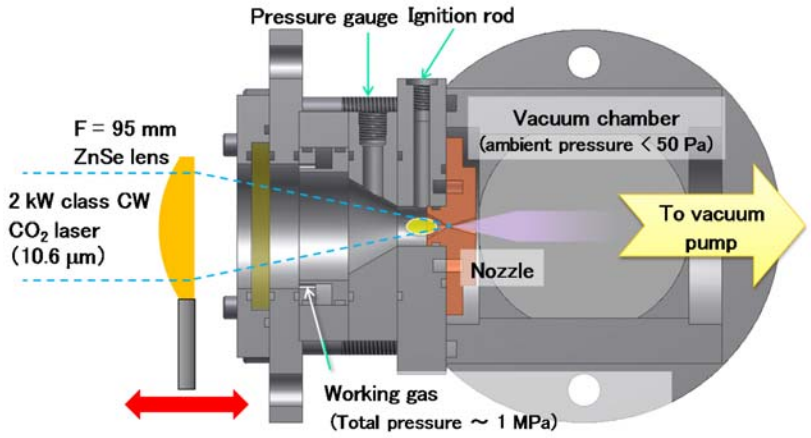

Fig. 1 Schematic of laser-driven plasma wind tunnel.

III. Measurement Methods

A. Principle of LAS

The flow velocity and translational temperature were measured by a diode-laser-based LAS system developed at the University of Tokyo [18, 19].

The relationship between the laser intensity and the absorption coefficient is expressed by the Beer Lambert law as

$$\frac{\mathrm{d}I(\nu,y)}{\mathrm{d}x} = -k(\nu,x,y)\,I(\nu,y). \tag{1}$$

Under our experimental conditions, Doppler broadening was on the order of several gigahertz, which is two orders of magnitude greater than all other broadenings, such as natural, pressure, and Stark broadenings. The absorption profile was approximated as a Gaussian profile as follows:

$$k(\nu,r)=\frac{2K(x)}{\Delta\nu_{\mathrm{D}}}\sqrt{\frac{\ln 2}{\pi}}\exp\left[-\ln 2\left\{\frac{2(\nu-\nu_0-\nu_{\mathrm{shift}})}{\Delta\nu_{\mathrm{D}}}\right\}^2\right] \tag{3}$$

The shift of the center absorption frequency by the Doppler effect is related to the flow velocity as

$$\nu_{\mathrm{shift}}=\frac{u\nu_0}{c}\sin\theta. \tag{5}$$

The Doppler width is the full width at half maximum of the profile and is related to the translational temperature as

$$\Delta\nu_{\mathrm{D}}=2\nu_0\sqrt{\frac{2k_{\mathrm{B}}T}{mc^2}\ln 2}. \tag{4}$$

The target line was the absorption from the meta-stable state of atomic oxygen at 777.19 nm.

B. LAS measurement system

Figure 2 shows a schematic of the LAS measurement system. A distributed-feedback (DFB) diode laser (DFB-076083, nanoplus GmbH) with a line width of less than 1 MHz was used as the laser oscillator. The laser frequency was scanned over the absorption shape. The modulation frequency and width were 3 kHz and 30 GHz, respectively. An etalon with a free spectral range of 0.75 GHz was used to calibrate the relative frequency. A microwave discharge oxygen plasma was used as a stationary plasma source to calibrate the center absorption frequency.

The probe beam, with a diameter of 1 mm at the chamber center, was guided to the chamber window through an optical fiber. The fiber output with a collimate lens was mounted on a one-dimensional traverse stage to scan the flow in the radial direction. To reduce plasma emission, the transmitted laser intensity was measured by a photodetector (PD; DET110/M, Thorlabs, Inc.) at a distance of 2 m from the chamber window. The PD was equipped with a 2-mm pinhole and a band-pass filter (BPF) having a full width at half maximum of 10 nm (FB770-10, Thorlabs, Inc.). The plasma emission was monitored by a PD and used as a trigger for data acquisition. All signals were recorded using a digital oscilloscope with 16-bit resolution at a sampling rate of 10 MHz (DL708; YOKOGAWA Co.). The measurement plane was 15 mm downstream from the nozzle exit, and the incident laser beam angle was 5.0°.

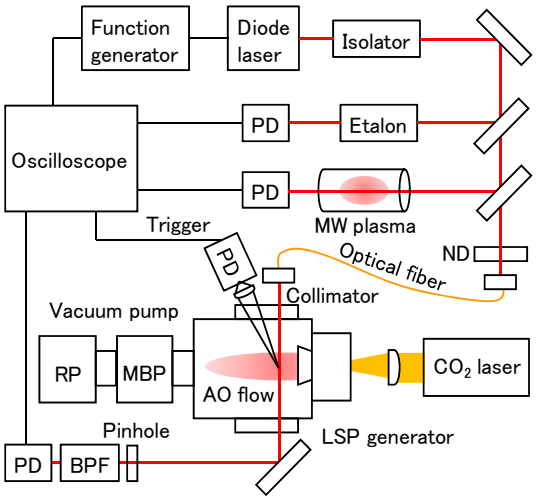

Fig. 2 Schematic of LAS measurement system.

IV. Results and Discussion

A. Generation conditions

Figure 3 shows the minimum laser power required for the generation of oxygen LSP as a function of plenum pressure. For comparison, the minimum laser power of argon is also plotted. Here, the pressure values are those for cold gases. The minimum laser power required for oxygen is higher than that for argon, because the dissociation energy is necessary for oxygen in addition to the ionization energy to generate enough electron density to maintain the LSP. For both gases, the LSP could be generated with higher laser power at lower pressure. The flow velocity is expected to be higher at higher specific enthalpy. However, in addition to the laser power, the operation pressure required for LSP generation is a limiting factor for the minimum mass flow rate. Then, in this study, the nozzle throat diameter was reduced to maintain a suitable operation pressure for a lower mass flow rate and higher specific enthalpy.

After the operation in these conditions, the plenum pressure for cold gases almost kept as much as before. This result shows that the throat area was little increased due to the erosion, which means the contamination in the flow was very low even if the pure-oxygen operation. In fact, as a result of emission spectroscopy for the plume, the emission intensity of Cu I 521.82 nm could not be detected whereas the strong OI 777.19 nm intensity was detected. The low erosion would be caused by following LSP characteristics. Since the LSP is produced by a focused laser

beam on the axis, it has the steep temperature distribution in the radial direction, resulting in the relatively low temperature near the throat wall [20].

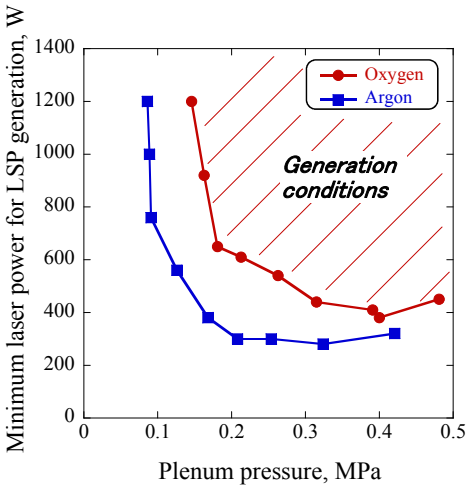

Fig. 3 Minimum laser power for oxygen and argon LSP generation versus plenum pressure.

B. Pure oxygen flows

1. Influence of plasma oscillation on flow properties

Figure 4 shows a photograph of a pure oxygen flow and measurement position. The LSP was moved as close as possible to the nozzle throat to maximize the emission region of the plume at an axial resolution of 0.2 mm. In our previous study [21], the emission intensity was found to fluctuate owing to a 2% variation of the laser power. Then, in this study, the influence of the LSP oscillation on the time variation of the flow characteristics was first evaluated.

Figure 5 shows typical transmitted laser intensity in the plume and the reference microwave plasma and etalon signals. The time variations of the flow velocity and translational temperature was estimated from the measured Doppler shift and width. Figure 6 shows the time variation of the flow velocity and emission intensity. Here, the error bar shows the standard deviation of ten measurements. As seen in this figure, the flow velocity does not entirely coincide with the emission intensity and has a variation of just several percent, whereas the variation of the emission intensity is 47 %. The variation of the translational temperature is also about 10%. Since the time variation of the absorption profiles off the axis was too small to be detected completely, we focused on the time-averaged flow properties on the axis without Abel inversion.

2. Time averaged flow properties

Figure 7 shows the plot of the time-averaged flow velocity versus the variation of the nozzle throat diameter. The mass flow rate was minimized in order to maximize the specific enthalpy. The laser power was fixed to 1300 W. As seen in this figure, the velocity increased with an increase in the specific enthalpy. The maximum flow velocity of 6.1 ± 0.96 km/s was achieved at the plenum pressure of 227 kPa and ambient pressure of 28.3 Pa. Under this condition, the translational temperature was 1216 ± 139 K. This value corresponds to an atomic thermal energy of 0.1 eV in LEO. At smaller throat diameters, the alignment between the laser beam and the throat axis degrades. This causes a larger alignment error, resulting in an increase in the error bar for smaller throat diameters.

3. Flux density of atomic oxygen

Under the assuming of an isentropic expansion and chemically frozen flow through the nozzle expansion, the total specific enthalpy is expressed as

$$\begin{aligned} h_0 &= \frac{1}{2}\gamma RT^* + \int_{T_{ref}}^{T^*} C_p dT + h_{chem} \qquad \text{(Throat)} \\ &= \frac{1}{2}u^2 + \int_{T_{ref}}^{T} C_p dT + h_{chem} \qquad \text{(Plume)} \end{aligned} \quad . \tag{5}$$

Since the plenum pressure is high enough to assume thermochemical equilibrium, the throat temperature and chemical composition can be calculated by the measured velocity and the temperature in the plume. Then, the throat temperature was estimated as being 11460 K and the mole fraction of atomic oxygen was found to be 0.98 in the plume. The total number density in the plume can be estimated from the temperature and ambient pressure using an equation of state. Then, the flux density of the atomic oxygen was estimated as 1.0×10^{25} atom/m^{2}s, which is more than four orders of magnitude larger than that in the LEO. Therefore, the developed wind tunnel can simulate atomic oxygen dosage over 1 day in the LEO in just 12 s. However, to match the flux density to the LEO environment, a vacuum pump with a higher exhaust velocity is required. Another different condition is that the rest mole fraction of 0.02 is atomic oxygen ion. Then, if it disturbs material tests, a magnetic filter would be necessary to remove it.

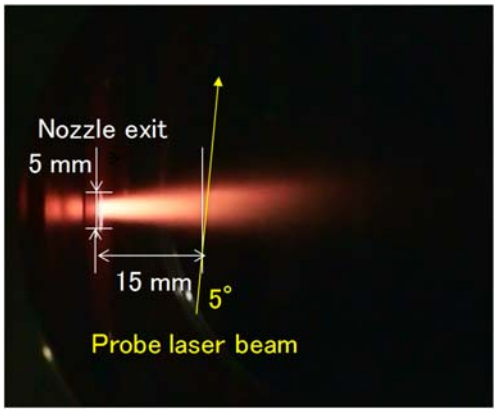

Fig. 4 Photograph of pure oxygen flow.

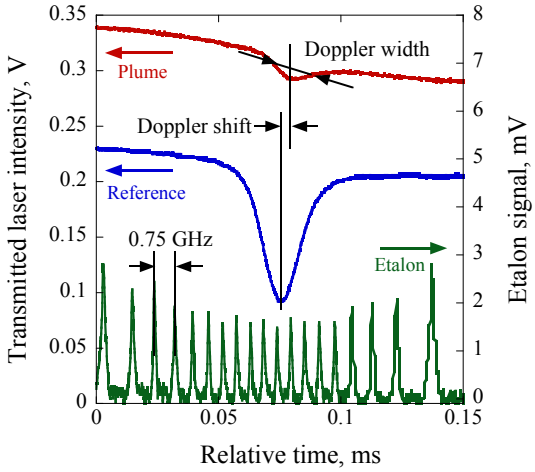

Fig.5 Typical signals.

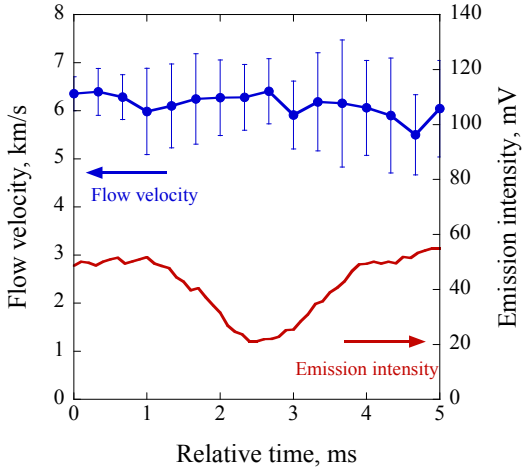

Fig. 6 Time variations of flow velocity and emission intensity.

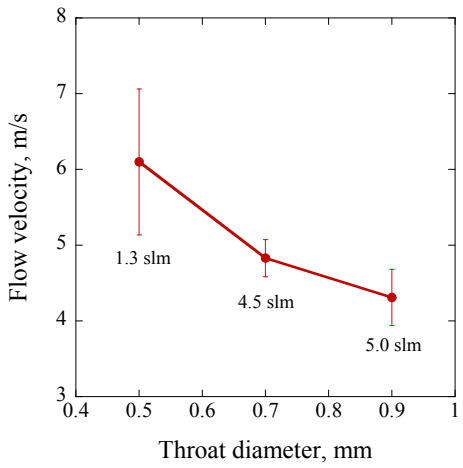

Fig. 7 Flow velocity as a function of throat diameter.

C. Oxygen/helium mixed flows

Even if the flow is properly expanded to room temperature, the increase in the velocity estimated by the equation $u(T_{\mathrm{room}}) = \sqrt{u^2(T) + \int_{T_{\mathrm{room}}}^{T} C_{\mathrm{p}} dT}$ is just 0.1 km/s for u = 6.1 km/s and T = 1216 K. Theoretically, to achieve the orbital velocity of 7.8 km/s, the throat temperature should be increased to 17000 K. However, this condition is difficult to achieve because the radiation loss increases with the cube of the temperature, in addition to obviously including severe thermal conditions.

Then, to resolve this problem, helium was mixed with oxygen to increase the flow velocity through a reduction in the average molecular weight, because velocity is related to average molecular weight as

$$u \propto \sqrt{\frac{T_0}{M_{\mathrm{av}}}} \tag{6}$$

Figure 8 shows the flow velocity as a function of the average molecular weight at a laser power of 1300 W and a fixed total mass flow rate of 1.3 slm. LSP could not be generated at a higher helium mole fraction of 0.23, because the ionization energy of helium is much higher than that of oxygen. As seen in this figure, velocity increased with increasing helium mole fraction. The maximum velocity was 6.6 ± 0.52 km/s corresponding to a helium mole fraction of 0.23. The velocity increase is well fitted to Eq. (6). Then, this velocity would be sufficient for achieving an orbital velocity of 7.8 km/s corresponding to the helium mole fraction of 0.58, though a higher laser power is necessary to generate LSP under this condition.

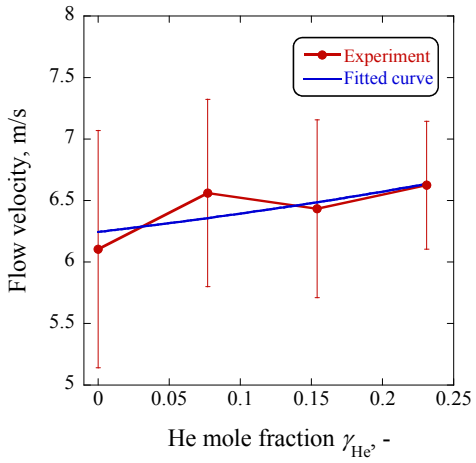

Fig. 8 Flow velocity as a function of helium mole fraction.

V. Conclusion

A laser-driven plasma wind tunnel was developed in this study as a simulator of high-speed continuous atomic oxygen flows in the low earth orbit environment. Laser diagnostics of the plume revealed the time-averaged flow velocity and translational temperature of the flows to be 6.1 ± 0.96 km/s and 1216 ± 139 K, respectively. The flux density for pure oxygen flows was estimated as 1.3×10^{25} atom/m^{2}s. The flow velocity could be increased to 6.6 ± 0.52 km/s by mixing oxygen with helium at a mole fraction of 0.23. An orbital velocity of 7.8 km/s could be achieved by increasing the helium mole fraction to 0.58.

Acknowledgments

This research was partially supported by the Ministry of Education, Culture, Sports, Science and Technology, a Grant-in-Aid for Young Scientists (A), 22686079, 2010, and a Grant-in-Aid for Scientific Research (B) 25289302, 2013.

References

[1] Smith, R. E., and Anderson, B. F., "Natural Orbital Environment Guidelines for Use in Aerospace Vehicle Development," NASA TM-4527, 1994.

[2] Silverman, E. M., "Space Environmental Effects on Spacecraft: LEO Materials Selection Guide," NASA CR-4661, 1995.

[3] Leger, L. J., and Visentine, J. T., "A Consideration of Atomic Oxygen Interactions with the Space Station," *Journal of Spacecraft and Rockets*, Vol. 23, No. 5, pp. 505–511, 1986.

[4] Ozaki, T., Osuga, H., Nagano, H., Hayakawa, Y., and Kajiwara, K., "Development Status of Ion Engine for Air Drag Compensation of SLATS," *47th AIAA/ASME/SAE/ASEE Joint Propulsion Conference & Exhibit*, AIAA Paper 2011-6072, 2011.

[5] Steiger, C., Costa, A. D., Emanuelli, P. P., Floberghagen, R., and Fehringer, M., "Evolution of Flight Operations for ESA's Gravity Mission GOCE," *SpaceOps 2012 Conference*, 2012. doi: 10.2514/6.2012-1262715

[6] Pekker, L., and Keidar, M., "Analysis of Airbreathing Hall-Effect Thrusters," *Journal of Propulsion and Power*, Vol. 28, No. 6, 2012, pp. 1399–1405.

[7] Garrigues, L., "Computational Study of Hall-Effect Thruster with Ambient Atmospheric Gas as Propellant," *Journal of Propulsion and Power*, Vol. 28, No. 2, 2012, pp. 344–354.

[8] Tagawa, M., Yokota, K., Nishiyama, K., Kuninaka, H., Yoshizawa, Y., Yamamoto, D., and Tsuboi, T., "Experimental Study of Air Breathing Ion Engine Using Laser Detonation Beam Source," *Journal of Propulsion and Power*, Vo. 29, No. 3, 2013, pp. 501–506.

[9] Caledonia, G., Krech, R. H., and Green, B. D., "A High Flux Source of Energetic Oxygen Atoms for Material Degradation Studies," *AIAA Journal*, Vol. 25, No. 1, 1987, pp. 59–63.

[10] Tagawa, M., Tomita, M., Umeno, M., and Ohmae, N., "Atomic Oxygen Generators for Surface Studies in Low Earth Orbit," *AIAA Journal*, Vol. 32, No. 1, 1994, pp. 95–100.

[11] Maldonado, C. A., Ketsdever, A., Rand, L. P., Xie, K., Farnell, C., Williams, J. D., "Characterization of an Atomic Oxygen Plasma Source for Ground-Based Simulation of the LEO Neutral Environment," *5th AIAA Atmospheric and Space Environments Conference*, AIAA Paper 2013-2681, 2013.

[12] Dodd, J. A., Baker, P. M., Hwang, E. S., Sporleder, D., Steams, J. A., Shambreau, S. D., Braunstein, M., and Conforti, P. F., "Hyperthermal Atomic Oxygen Source for Near-Space Simulation Experiments," *Review of Scientific Instruments*, Vol. 80, No. 9, 2009, 093104.

[13] Matsui, M., Komurasaki, K., and Arakawa, Y., "Sensitivity Enhancement of Laser Absorption Spectroscopy for Atomic Oxygen Measurement in Microwave Air Plasma," *Vacuum*, Vol. 83, Nos. 1–4, Sept. 2008, pp. 21–24.

[14] Matsui, M., Ikemoto, T., Takayanagi, H., Komurasaki, K., and Arakawa, Y., "Generation of Highly Dissociated Oxygen Flows using a Constrictor-Type Arc-Heater," *Journal of Thermophysics and Heat Transfer*, Vol. 21, No. 1, 2007, pp. 247–249.

[15] Matsui, M., Takayanagi, H., Oda, Y., Komurasaki, K., and Arakawa, Y., "Performance of Arcjet-Type Atomic-Oxygen Generator by Laser Absorption Spectroscopy and CFD analysis," *Vacuum*, Vol. 73, Nos. 3–4, 2004, pp. 341–346.

[16] Matsui, M., Tanaka, K., Nomura, S., Komurasaki, K., Yamagiwa, Y., and Arakawa, Y., "Generation and Diagnostics of Atmospheric Pressure CO_2 Plasma by Laser Driven Plasma Wind Tunnel," *Journal of Applied Physics*, Vol. 112, 2012, 033301.

[17] Matsui, M., Shinmi, K., Ueno, T., Komurasaki, K., and Arakawa, Y., "Operation Characteristics of Laser Driven Plasma Wind Tunnel," Transactions of Space Technology Japan, Vol. 7, No. ISTS26, 2009, pp. 31–39.

[18] Matsui, M., Komurasaki, K., Herdrich, G., and Auweter-Kurtz, M., "Enthalpy Measurement in Inductively Heated Plasma Generator Flow by Laser Absorption Spectroscopy," *AIAA Journal* Vol. 43, No. 9, 2005, pp. 2060–2064.

[19] Matsui, M., Ogawa, S., Komurasaki, K., and Arakawa, Y., "Influence of Laser Intensity on Absorption Line Broadening in Laser Absorption Spectroscopy," *Journal of Applied Physics*, Vol. 100, 2006, 063102.

[20] Nakano, N., "Numerical Simulation of a 1 kW-Class CW Laser Thruster," Transactions of the Japan Society for Aeronautical and Space Sciences, Vol. 49, No. 166, 2007, pp. 211-219.

[21] Inoue, T., Ijiri, T., Hosoda, S., Kojima, K., Uehara, S., Komurasaki, K., Arakawa, Y., "Oscillation Phenomenon of Laser-Sustained Plasma in a CW Laser Propulsion," *Vacuum*, Vol. 73, 2004, pp.433–438.